

Green Chemistry

Accepted Manuscript

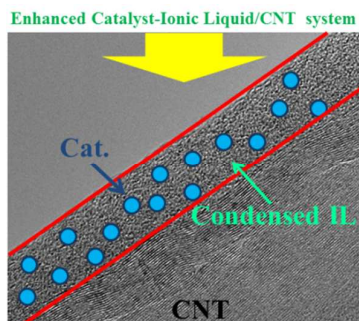


This is an *Accepted Manuscript*, which has been through the Royal Society of Chemistry peer review process and has been accepted for publication.

Accepted Manuscripts are published online shortly after acceptance, before technical editing, formatting and proof reading. Using this free service, authors can make their results available to the community, in citable form, before we publish the edited article. We will replace this *Accepted Manuscript* with the edited and formatted *Advance Article* as soon as it is available.

You can find more information about *Accepted Manuscripts* in the [Information for Authors](#).

Please note that technical editing may introduce minor changes to the text and/or graphics, which may alter content. The journal's standard [Terms & Conditions](#) and the [Ethical guidelines](#) still apply. In no event shall the Royal Society of Chemistry be held responsible for any errors or omissions in this *Accepted Manuscript* or any consequences arising from the use of any information it contains.



A new concept of ionic liquid mono-dispersing catalyst on nanocarbon surface is presented with enhanced catalytic activity.

EDGE ARTICLE

Heterogenization of Homogenous Reaction System on Carbon Surface with Ionic liquid as mediator

Cite this: DOI: 10.1039/x0xx00000x

Yuxiao Ding, Bingsen Zhang, Neeraj Gupta and Dang Sheng Su*

Received 00th January 2012,

Accepted 00th January 2012

DOI: 10.1039/x0xx00000x

www.rsc.org/

A new concept of ionic liquid (IL) mono-dispersing catalyst on nanocarbon surface is presented. The liquid mixture of IL and model catalyst (1-octyl-3-methyl imidazolium phosphotungstate, OPW) on carbon nanotube is in solid state which can be easily characterized and give a fundamental understanding of the interaction between the catalyst and the IL. The condensed IL is found to weaken the W=O bond of catalyst that favours its interaction with oxidizing agent, that exhibited a reaction rate of 176 times to the performance of single OPW during the oxidation of dibenzothiophene. Due to the heterogenization of this system, the catalyst can be easily recycled by a simple gravity separation.

Introduction

In spite of their numerous benefits, many homogeneous processes are not used at industrial scale because of few obstacles, such as the separation of the products, the need for organic solvents, and inability for recycling of catalyst.^{1,2} Ionic liquids (ILs), with their ionic nature, polarity, low-volatility and thermal stability, have gained a lot of attraction by providing a liquid-liquid biphasic catalysis system to address these difficulties.³⁻⁷ The concept of this biphasic catalysis implies that the catalyst is soluble in IL phase whereas the substrates remain in the other phase, endowing the system with advantages of both homogeneous and heterogeneous catalysis.⁸ However, the IL-organic systems require large amounts of ILs, which lower their cost-effectiveness since ILs are too expensive. To solve this problem, a variety of reactions have been studied through the immobilization of molecular catalysts in supported IL phases.^{9, 10} Catalyst, ILs and solid supports can combine in various ways to reduce the amount of IL, and the combination makes the separation of catalyst from reaction substrates phase easier. In most cases supports used in the immobilization process are of high surface area and large pore volume such as porous silica gels.^{11, 12} The main preparation method is impregnation, that uses volatile organic solvent to dissolve the catalyst and IL.¹³ Then the solution is mixed with support materials and the volatile solvent is removed by evaporation under reduced pressure. Undoubtedly, the supported catalysts by impregnation are ideally suitable for gas phase catalysis. Nevertheless, catalyst can leach out of the IL phase when it is used under the liquid phase condition. Covalently anchored IL with functional groups such as -COOH, -NH₂, -OH fragments

can well improve their stability in liquid phase catalysis.^{14, 15} However, compared to impregnation this method has more restrictions on the IL structure, such as presence of few functional groups that make them even more expensive. Also, the preparation process becomes more complicated.

CNTs have found applications as supports in catalysis and have also been proved on enhancing the electron-transfer rate in many redox reactions.¹⁶ Recently, it is reported that imidazolium ILs can have a strong non-covalent interaction with graphitic surface of CNTs.¹⁷⁻²⁰ Herein, by using the volatility^{21, 22} of ILs at low pressure, we propose a physical method to exfoliate ILs layer by layer and obtain a condensed IL phase on CNT surface. Different ILs can be condensed in this process to immobilize different kinds of catalysts on heterogeneous CNT. The catalytic reaction will homogeneously happen in this nano-scale condensed IL, while the IL will enhance the reaction rate. In addition, the thin layers of the IL make the mass transfer of fast chemical reactions or gas phase reactions unlimited.

With this strategy, a tungsten-based polyoxometalate OPW ([Omim]₃PW₁₂O₄₀) was chosen as a model catalyst because of the wide interest of polyoxometalates in their use of redox reaction.²³⁻²⁶ Our approach is based on the non-covalent interaction between imidazolium IL 1-octyl-3-methyl imidazolium hexafluorophosphate (OmimPF₆, denoted as OP) and high-temperature-treated highly graphitic CNT (HHT, a type of MWCNTs treated at 3000 °C to obtain very high graphitization degree that can exclude the influence of metal impurities, defects and oxygen functional groups on CNT surface). OPW was dispersed in OP at 120 °C forming a homogeneous mixture and then it was fabricated on the HHT

surface to form OPW-OP/CNT gel. Finally, the bulk IL phase was exfoliated layer by layer to obtain a homogeneously condensed OPW-OP (as shown in Figure 1). The OPW can be highly dispersed in the OP layer and the hydrogen bond network of the IL can prevent their agglomeration during the heating and reaction processes. Besides, the strong π - π interaction between CNTs is shielded by the ILs, preventing the detached CNTs from rebundling.²⁷ The catalytic system was then applied to the oxidation of dibenzothiophene (DBT), providing enhanced efficiency and easy recovery.

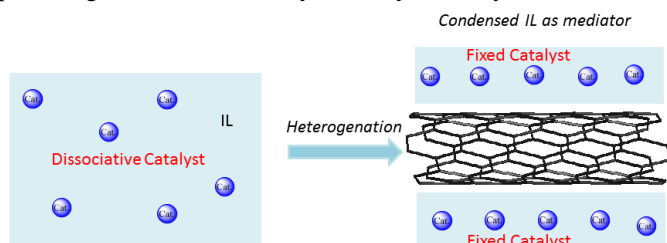


Figure 1. Schematic illustration of the fabrication of the OPW-OP/HHT nanocomposites.

Results and discussion

As annealing treatment is needed for the synthesis of the catalyst, the thermo-stability of the IL, polyoxometalate and the precursor in this annealing process are important. In general, the mass loss of any liquid during a heating treatment may contain evaporation and thermal decomposition simultaneously.^{28, 29} Mostly, the decomposition is more sensitive to temperature, and thus decomposition (evaporation) may dominate the overall mass loss, if high (low) heating rates are used. Due to a thermogravimetric (TG) experiment is usually last a short period, and thus the real critical temperature is passed through relatively quickly without a measurable mass loss.^{30, 31} Therefore, TG only shows comparative values of different samples here, but not gives an exact decomposition temperature. TG (Figure 2a) curves of OP and OPW indicate that the weight loss began at 344 °C and 392 °C respectively. However, the mixture shows a lower decomposition temperature at 300 °C and a slight weight loss (3%) before 310 °C which can be attributed to the decomposition of IL anion. TPD results of OPW-OP/HHT gel (Figure 2b) are consistent with the conclusion mentioned above. Only F^+ and HF can be detected at 280 °C, while after 310 °C alkyl debris can be detected that produced by cation decomposition of the OPW-OP/HHT gel (Figure 2c). The decomposition of imidazolium cation can be attributed to OP cation (under yellow shadow) and OPW cation respectively. This demonstrates that the hybrid of OP and OPW is only mechanically mixed without forming a new compound, so that the choice of polyoxometalate positive ion is more flexible. The molecular interactions of pristine OP or OPW, such as hydrogen bond, make the decomposition of their pure material

difficult.^{32, 33} The introduction and dispersion of OPW molecules in OP destroy the hydrogen bond network of the IL, leading to an easier decomposition of both OP and OPW. On the contrary, the strong interaction between IL and CNT, which has been proved as the static-assistant CH- π hydrogen bond, brings an obvious TG shift to higher temperature from former work.^{34, 35} The endothermic peak of polyoxometalate DSC curve (Figure S1) at 605 °C was generated by the thermogravimetric behavior of OPW anion that proved the stability of OPW anion before 570 °C.

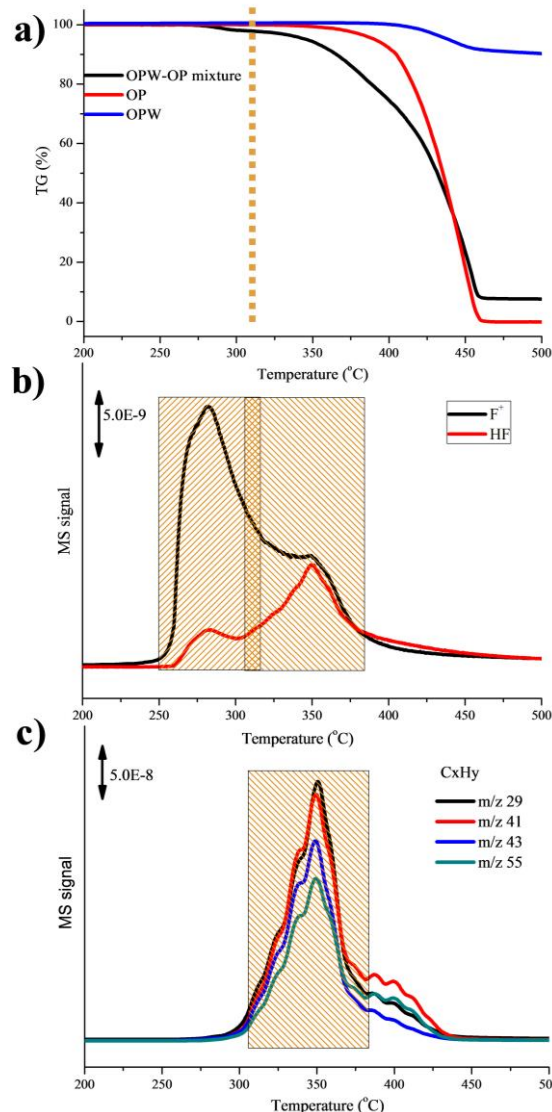


Figure 2. a) TG-DSC curves of pristine IL, OPW and OPW-OP mixture, b) TPD profiles of OPWIL/HHT gel: F element attribution of the anion decomposition, c) TPD profiles of OPWIL/HHT gel: CxHy attribution of the cation decomposition.

The ESI-MS spectra of the negative ion of pristine IL and OPW-IL/HHT nanocomposites are given in Figure S2. Interestingly, most IL still exist as dimer or multimer even in a polar solvent acetonitrile because of its strong hydrogen

network (Figure S2a). However, with the introduction of OPW into the IL most of these multimers disappear (Figure S2b), which means OPW molecules uniformly merged into the hydrogen bond network of IL and reduced the ions interaction of IL. ESI-MS spectra of positive ions (Figure S3) show the slight change caused by the annealing process. Only m/z signal 195.2 for the Omim⁺ cation and 535.0 for the Omim⁺[OmimPF₆] cation could be detected in the pure IL; while after the annealing process a small amount of cation impurities were observed at m/z 209.2, 490.6 and 782.9. However, the amount of the impurities was so small that the properties of OP were maintained.^[10a] No signal corresponding to tungsten-containing ion impurities signals are observed in both negative and positive ion spectrum of the OPW-OP/HHT nanocomposites, which proved that the annealing treatment has no influence on the OPW.

Due to their inertness, the inherent smooth graphite surface always results in very weak interfacial interactions between CNTs and the ordinary supported catalyst (like palladium and iridium). The active sites of carbon materials such as the oxygen, nitrogen functional groups or defects are always needed to adsorb these catalysts. Contrary to these ordinary supporting catalysts, the OPW was first homogeneously dissolved into the IL and thus did not depend much on the affects of carbon surface. In the synthesis process, ILs not only act as bridge for OPW and CNT surface, but also act as homogeneous media for OPW mono-dispersion. CNT is a rare example that can form stable IL-carbon nanocomposites with non-covalent force, mostly the static-assistant CH- π hydrogen bond.³⁴ In Figure 2c, we can see a series of shoulder peaks that indicate increased interaction between the CNT surface with different IL layers. This provides a simple way to exfoliate IL on CNT surface layer by layer.

High-resolution transmission electron microscopy (HRTEM) was used to reveal the structure of OPW-OP/HHT. Uniform IL coating about several nanometers can be intuitively observed on the surface of the OPW-OP/HHT (Figure 3a), while for the pristine HHT (Figure S4) only a smooth surface is observed. High angle annular dark field-scanning TEM (HAADF-STEM) image of OPW-OP/HHT nanocomposite (Figure S5) exhibits uniformly dispersed small white point of OPW molecules with about 1 nm diameter on the HHT surface indicating that OPW has mono-dispersed in the condensed IL coating. The STEM-EDS elemental mappings (Figure 3b, c) also show that all the contained species such as N, P, F, W, and O are uniformly dispersed on the HHT surface. From the TEM results, the exfoliating process has no influence on OPW dispersion and the structure is maintained well. For the use of graphitic surface to form non-covalent bond with IL, the CNT can be substituted with other nanocarbon such as graphene, graphite, carbon nanofiber and so on. The IL mediator can also be extended to tune all kinds of other catalytic properties, due to their ability to dissolve many inorganic salts and diverse nature

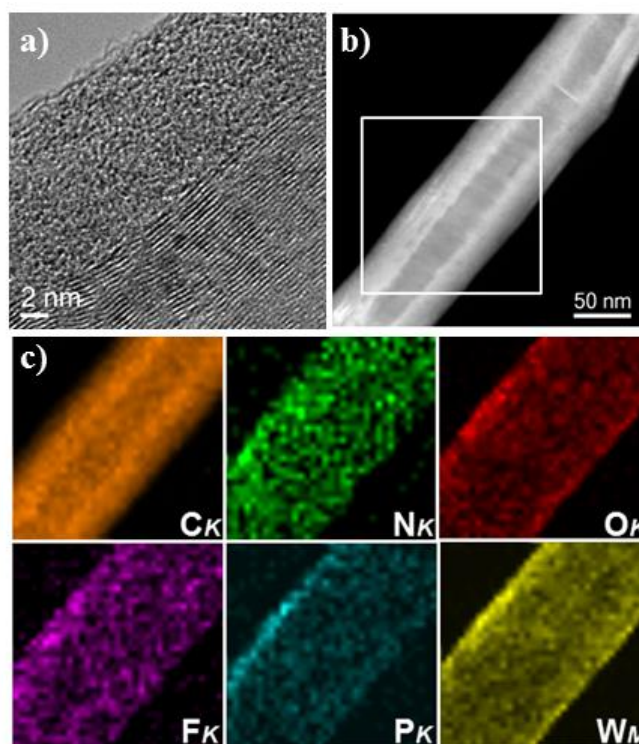


Figure 3. a) HRTEM, b) HAADF-STEM and c) Element mapping images of the OPW-OP/HHT nanocomposites (the mapping was obtained in white square of b).

The interactions between the catalyst and IL in biphasic catalysis are always hard to prove due to the continuous movement of molecules. But the solid nature of OPW-OP on HHT surface makes it easy for different characterizations to obtain the detailed informations about their interactions. X-ray diffraction (XRD) of OPW is quite complicated (Figure S6) but no signal of OPW can be observed in the pattern of OPW-OP/HHT, which illustrates that the polyoxometalate have dispersed nicely in the IL layers without aggregation of OPW molecules during the annealing process. The diffuse-reflectance infrared fourier transform (DRIFT) spectra were used to detect structural and bonding changes of the OPW and OP in their hybrid on HHT surface. In Figure S7, the spectrum of OPW conforms the parent PW₁₂O₄₀³⁻ Keggin structure which shows characteristic P–O stretching (~1083 cm⁻¹), W–O terminal stretching (~987 cm⁻¹), stretching of W–O–W inter bridges between corner-sharing WO₆ octahedra (~891 cm⁻¹) and stretching of W–O–W intra bridges between edge-sharing WO₆ octahedra (~815 cm⁻¹). The DRIFT spectrum of OPW-OP mixture shows the same result with pristine IL and OPW, which proves that the mixing process has no influence on their structures. The main peaks of the OPW in the OPW-OP/HHT system are maintained after the annealing treatment. The peak changes in the green dash area can be attributed to the slight decomposition of the IL. About 30 cm⁻¹ red shift of W–O vibration might be caused by the condensation of IL (from liquid phase to the solid phase) leading to a micro environment change of OPW. The interaction between ILs and catalysts is

difficult to be determined in liquid phase. The formed catalyst-IL/HHT powder not only can fix this problem, but also enhance their interaction through condensed IL. The red shift of OPW can only be observed in condensed IL as shown in DRIFT results, which is caused by the weakening W=O bond in IL. Obviously, the condensed IL not only brings convenience for the characterization of the IL-catalyst system, but also endows much better catalytic ability than pristine OPW. The weakened W=O bond favors the formation of WO_2 peroxide.

The binding energy of the core level in the X-ray photoelectron spectroscopy (XPS) shifts due to the shielding effect of outer electrons, so the binding energy (peak position) of tungsten in OPW is related to its chemical environments. Figure 4a shows XPS spectra of the pure OPW and OPW-OP/HHT. In comparison to pure OPW, two peaks of W4f in nanocomposites shift about 0.7 eV to lower binding energy, which is most likely due to the high electronegativity of IL anion influencing the W=O bond. The lower binding energy of W makes it easier to react with oxidizing agent that can explain the reason for the high efficiency of polyoxometalates in the oxidation reaction with IL.³⁶

Figure 4b gives DBT conversion, turn over frequency (TOF) and mass-specific activity (MSA) of different catalysts in DBT oxidation process (see detail calculation information in SI). It shows that HHT has almost no catalytic activity for the oxidant H_2O_2 . The single OPW shows $0.5 \times 10^{-2} \text{ min}^{-1}$ MSA value due to its low dispersion in the reaction system. Highly dispersed OPW/HHT (see SI) and OPW-OP/HHT show much higher MSA results, about 13 and 176 times to the performance of single OPW, respectively. Although both of them are highly dispersed on the HHT surface, OPW-OP/HHT shows higher TOF ($87.9 \times 10^{-2} \text{ min}^{-1}$) than that of OPW/HHT ($6.5 \times 10^{-2} \text{ min}^{-1}$). This demonstrates the superiority of IL mediator proven by XPS that the condensed IL lowers the binding energy of W4f electron and thus making it easier to react with oxidizing agent. Concomitantly, the strong hydrogen bonding between OP and DBT³⁷ partially destroyed the aromaticity of DBT and thus the oxidation takes place easily in the presence of IL.³⁸ ILs have been widely proved to have promoting effect for the catalytic efficiency, but their amount is always large.³⁶ For the DBT conversion in other reported works, 1 ml to 3 ml IL is necessary for 5 ml solvent to achieve a deep oxidation. Herein, only 20 mg OPW-OP/CNT system can achieve the same results indicating that the condensed IL (lower than 1% IL in liquid phase) on CNT surface possess much more positive influence than the bulk liquid IL. CNT also favors the introduction of the reactant into the IL reactor due to the π - π interaction between CNT and DBT. During the course of oxidation process using IL the unwanted “contamination” of the solvent with OP was investigated. After the reaction, no IL was detected in the solvent with HPLC indicating the stability of formed catalyst system during the reaction. Figure S8 displayed the influence of the reaction temperature and time on the DBT conversion in the IL mediator. The activity of catalytic system improved with the increasing of temperature from 30 °C to 60 °C. The results demonstrate that the catalyst can work more efficiently with

H_2O_2 at higher temperatures. For the lower temperature, the DBT conversion still could reach a high level by prolonging the reaction time.

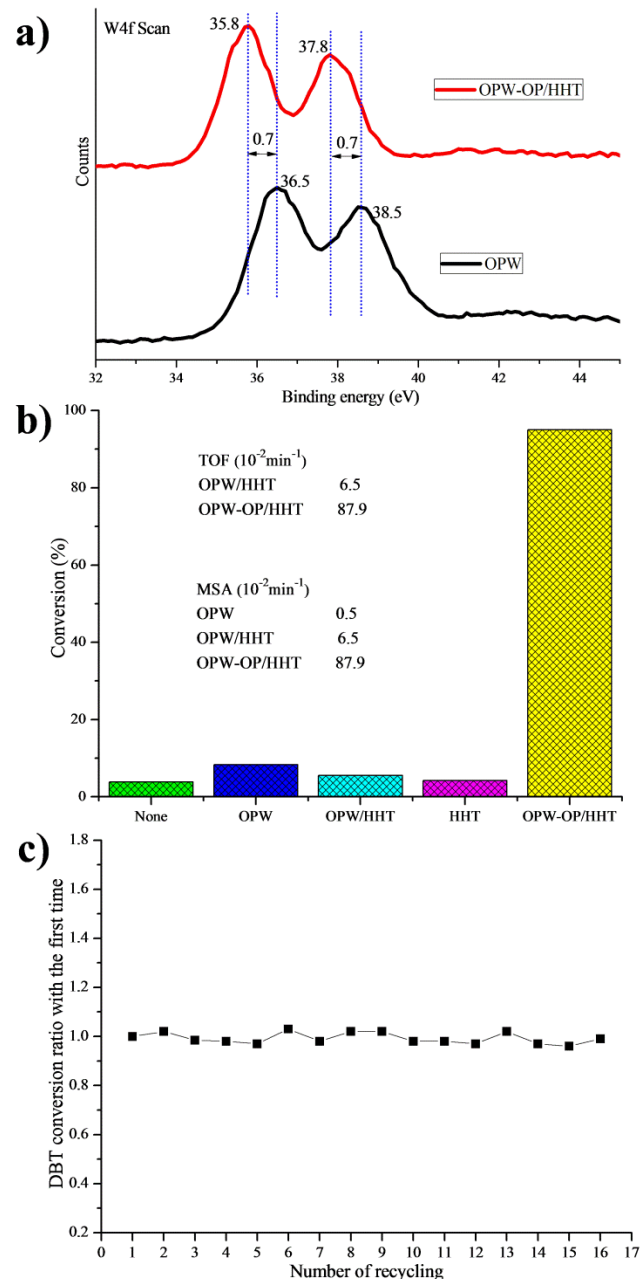


Figure 4. a) W4f XPS spectra of pure OPW and OPW-OP/HHT nanocomposites, b) DBT conversion with same amount of catalysts, TOF and MSA of different catalyst systems. Experimental conditions: $T = 60 \text{ }^\circ\text{C}$, $V(\text{H}_2\text{O}_2) = 24 \text{ }\mu\text{L}$, $m(\text{catalyst}) = 20 \text{ mg}$, $t = 40 \text{ min}$. TOF value was based on the <30% conversion, and given in mole of conversion of reactant per mole of OPW in the catalyst per hour. c) Cycling stability of the heterogeneous system. Experimental conditions: 5 mL model oil, $T = 60 \text{ }^\circ\text{C}$, $t = 40 \text{ min}$, $V(\text{H}_2\text{O}_2) = 24 \text{ }\mu\text{L}$, $m(\text{catalyst}) = 20 \text{ mg}$.

The regeneration and subsequent recycling of the catalyst are of vital importance for the industrial application of IL. The recyclability of liquid IL system is naturally less attractive. Figure 4c shows that the polyoxometalate in the IL phase are not aggregated or lost during the reaction process and therefore, the catalyst exhibits very good stability in recycling experiments. The heterogeneous CNT and the IL mediator favors the desorption of the oxidative products due to its high polarity,³¹ leaving enough space for the absorption of fresh reactant. Density of the heterogeneous catalyst system is much higher than n-octane, therefore it settle down easily and can be separated through decantation. Fresh H₂O₂ and model oil were added into the original reaction kettle for the next run. Although IL is very expensive for commercial application its exfoliation and solidification brings huge superiority for recycling experiments (Even after recycling 16 times, the system can reach high efficiency at par with its first use.). Meanwhile, the lower dosage of IL makes the use of polyoxometalate-IL system possible in industry applications.

Conclusions

In summary, we have developed a novel heterogenization process with IL as mediator on CNT surface. OPW in the condensed IL can be easily characterized thus giving a fundamental understanding of the interaction between the catalyst and IL. The condensed IL phase not only provides a homogenous reaction micro-environment but also lowers the binding energy of W4f electron leading to an easier reaction with oxidant. The catalyst in the condensed IL exhibits excellent oxidative activity for DBT oxidation, about 176 times MSA value to that of single OPW. Moreover, the catalyst in the IL mediator also shows high stability and the whole heterogeneous catalyst system can be regenerated by gravity separation (much easier and cheaper than filtration and centrifugation). With low dosage of IL and the superiority in catalytic redox reaction, this novel heterogenization process sheds a light of research on catalyst-IL interaction and goes a further step to bridge homogeneous-heterogeneous catalysis.

Experimental

Synthesis of OPW-OP/HHT

The OPW-OP/HHT was prepared as the following: 2.5 g IL ([Omim]PF₆, purchased from Alfa Aesar) and 0.2 g polyoxometalate (OPW, synthesized by the reported procedures) were mixed together and heated at 120 °C to disperse the polyoxometalate in IL phase. Then 0.23g HHT (a highly graphitic multi-walled CNT) was added into the mixture and ultrasonic treated for 50 minutes to disperse HHT in the mixture. The mixture was centrifuged at 9500 r/min. A transparent liquid phase, identified as the mixture, was separated from a black lower gel phase containing both mixture and CNTs. The black gel phase was removed to small quartz boats which were placed in the center of a larger alumina tube running through the center of a furnace. Temperature

programmed annealed processes were carried out according to the following procedures: annealing the IL and CNT gel from room temperature to 300 °C (10 Pa, 5 °C/min), maintaining for 60 min (10 Pa); then cooling it down to the room temperature in 2 h (10 Pa). The final products were obtained from the inside of the quartz boats after the annealing process. The oxidative procedure was run as follows: catalysts, 30% H₂O₂ and DBT (purchased from Sigma-Aldrich; solvent is n-octane, 500 ppm) were added into the two-neck kettle in turn, respectively. The mixture was then stirred under appropriate conditions. After the reaction, the kettle was cooled to room temperature and the oil was removed for further analysis via gas chromatography flame ionization detection (GC-FID) (Agilent 7890A, HP-5 column, 30 m long * 0.32 mm inner diameter (id) * 0.25 mm film thickness) (tetradecane as internal standard). The process started at 100 °C and the temperature was increased to 200 °C at a rate of 15 °C min⁻¹.

Surface and structure analysis

The TEM images and STEM-EDS elemental mapping were observed on a FEI Tecnai G2 F20 microscope operated at 200 kV. Thermogravimetric (TG) analysis was carried out using a NETZSCH STA 449 F3 under a flow of air (50 mL min⁻¹) with a heat ramp of 5 °C min⁻¹. XPS characterization was performed on an ESCALAB 250 instrument with Al K α X-rays (1489.6 eV). IR studies were conducted with a Thermo Nicolet iZ10 FTIR system using a diffuse reflectance infrared Fourier-transform (DRIFT) cell that has been extensively modified to allow in situ treatments up to 500°C under flowing gases. The spectra were recorded in the 650–4000 cm⁻¹ wavenumber range with 128 scans at a resolution of 4 cm⁻¹. X-ray diffraction (XRD) measurements were performed on a D/max 2400 diffractometer (JEOL Ltd., Japan) at a scanning rate of 4 °/min, with graphite monochromatized Cu K α radiation ($I = 0.1506$ nm).

Acknowledgements

The authors acknowledge the financial support from MOST (2011CBA00504), NSFC of China (21133010, 51221264, 21261160487), "Strategic Priority Research Program" of the Chinese Academy of Sciences, Grant No. XDA09030103. The authors are grateful to Prof. De Chen, Norwegian University of Science and Technology, for helpful discussions.

Notes and references

Shenyang National Laboratory for Materials Science, Institute of Metal Research, Chinese Academy of Sciences, Shenyang 110016, China. E-mail: dssu@imr.ac.cn

Electronic Supplementary Information (ESI) available: preparation of OPW/HHT, TG-DSC, ESI-MS spectra, TEM, wide angle XRD, DRIFT spectra and reaction data. See DOI: 10.1039/b000000x/

1. J. Dupont, R. F. de Souza and P. A. Z. Suarez, *Chem. Rev.*, 2002, **102**, 3667-3691.
2. M. Yoon, R. Srirambalaji and K. Kim, *Chem. Rev.*, 2012, **112**, 1196-1231.
3. J. P. Hallett and T. Welton, *Chem. Rev.*, 2011, **111**, 3508-3576.

4. P. Wasserscheid and W. Keim, *Angew. Chem.-Int. Edit.*, 2000, **39**, 3772-3789.
5. T. Welton, *Chem. Rev.*, 1999, **99**, 2071-2083.
6. R. Sheldon, *Chem. Commun.*, 2001, 2399-2407.
7. R. D. Rogers and K. R. Seddon, *Science*, 2003, **302**, 792-793.
8. K. R. Seddon, *Nat Mater*, 2003, **2**, 363-365.
9. L. J. Lozano, C. Godinez, A. P. de los Rios, F. J. Hernandez-Fernandez, S. Sanchez-Segado and F. J. Alguacil, *Journal of Membrane Science*, 2011, **376**, 1-14.
10. C. Van Doorslaer, J. Wahlen, P. Mertens, K. Binnemans and D. De Vos, *Dalton Transactions*, 2010, **39**, 8377-8390.
11. M. Massaro, S. Riela, G. Lazzara, M. Gruttadauria, S. Milioto and R. Noto, *Applied Organometallic Chemistry*, 2014, 234-238.
12. A. Riisager, R. Fehrmann, S. Flicker, R. van Hal, M. Haumann and P. Wasserscheid, *Angewandte Chemie International Edition*, 2005, **44**, 815-819.
13. J. Huang, T. Jiang, H. Gao, B. Han, Z. Liu, W. Wu, Y. Chang and G. Zhao, *Angewandte Chemie*, 2004, **116**, 1421-1423.
14. X. Zheng, S. Luo, L. Zhang and J.-P. Cheng, *Green Chem.*, 2009, **11**, 455-458.
15. M. H. Valkenberg, C. deCastro and W. F. Holderich, *Green Chem.*, 2002, **4**, 88-93.
16. B. Wu, D. Hu, Y. Kuang, B. Liu, X. Zhang and J. Chen, *Angewandte Chemie International Edition*, 2009, **48**, 4751-4754.
17. T. Fukushima, K. Asaka, A. Kosaka and T. Aida, *Angew. Chem.-Int. Edit.*, 2005, **44**, 2410-2413.
18. T. Fukushima, A. Kosaka, Y. Ishimura, T. Yamamoto, T. Takigawa, N. Ishii and T. Aida, *Science*, 2003, **300**, 2072-2074.
19. J. Lee and T. Aida, *Chem. Commun.*, 2011, **47**, 6757-6762.
20. J. J. Lee, A. Yamaguchi, M. A. Alam, Y. Yamamoto, T. Fukushima, K. Kato, M. Takata, N. Fujita and T. Aida, *Angew. Chem.-Int. Edit.*, 2012, **51**, 8490-8494.
21. M. J. Earle, J. Esperanca, M. A. Gilea, J. N. C. Lopes, L. P. N. Rebelo, J. W. Magee, K. R. Seddon and J. A. Widegren, *Nature*, 2006, **439**, 831-834.
22. P. Wasserscheid, *Nature*, 2006, **439**, 797-797.
23. Y. Leng, J. Wang, D. Zhu, X. Ren, H. Ge and L. Shen, *Angew. Chem.-Int. Edit.*, 2009, **48**, 168-171.
24. N. Mizuno, K. Yamaguchi and K. Kamata, *Coordination Chemistry Reviews*, 2005, **249**, 1944-1956.
25. A. Nisar, Y. Lu, J. Zhuang and X. Wang, *Angew. Chem.-Int. Edit.*, 2011, **50**, 3187-3192.
26. X. Zuwei, Z. Ning, S. Yu and L. Kunlan, *Science*, 2001, **292**, 1139-1141.
27. J. Y. Wang, H. B. Chu and Y. Li, *Acs Nano*, 2008, **2**, 2540-2546.
28. F. Heym, C. Kern, J. Thiessen and A. Jess, Wiley VCH, 97 - 104, 2014.
29. F. Heym, C. Kern, J. Thiessen and A. Jess, Wiley VCH, 105 - 143, 2014.
30. F. Heym, B. Etzold, J. Haber and A. Jess, *Phys. Chem. Chem. Phys.*, 2010, **12**, 12089 - 12100.
31. F. Heym, B. Etzold, C. Kern and A. Jess, *Green Chem.*, 2011, **13**, 1453-1466.
32. H. C. Chang, J. C. Jiang, W. C. Tsai, G. C. Chen and S. H. Lin, *J. Phys. Chem. B*, 2006, **110**, 3302-3307.
33. J. F. Huang, P. Y. Chen, I. W. Sun and S. P. Wang, *Spectrosc Lett*, 2001, **34**, 591-603.
34. Y. Ding and D. S. Su, *ChemSusChem*, 2014, 1542-1546.
35. Y. Ding, X. Sun, L. Zhang, S. Mao, Z. Xie, Z. W. Liu and D. S. Su, *Angew. Chem.-Int. Edit.*, 2014, DOI: 10.1002/anie.201408201R1.
36. Y. Ding, W. Zhu, H. Li, W. Jiang, M. Zhang, Y. Duan and Y. Chang, *Green Chem.*, 2011, **13**, 1210-1216.
37. M. H. F. Kox, K. F. Domke, J. P. R. Day, G. Rago, E. Stavitski, M. Bonn and B. M. Weckhuysen, *Angew. Chem.-Int. Edit.*, 2009, **48**, 8990-8994.
38. B. Zhang, Z. Jiang, J. Li, Y. Zhang, F. Lin, Y. Liu and C. Li, *Journal of Catalysis*, 2012, **287**, 5-12.